JOURNAL OF NEUROTRAUMA 34:248–256 (January 1, 2017)

DOI: 10.1089/neu.2015.4355

Abnormal Injury Response in Spontaneous Mild Ventriculomegaly Wistar Rat Brains: A Pathological Correlation Study of Diffusion Tensor and Magnetization Transfer Imaging in Mild Traumatic Brain Injury

Tsang-Wei Tu,[1] Jacob D. Lescher,[1] Rashida A. Williams,[1] Neekita Jikaria,[1] L. Christine Turtzo,[2] and Joseph A. Frank[1,3]

Abstract

Spontaneous mild ventriculomegaly (MVM) was previously reported in ~43% of Wistar rats in association with vascular anomalies without phenotypic manifestation. This mild traumatic brain injury (TBI) weight drop model study investigates whether MVM rats ($n = 15$) have different injury responses that could inadvertently complicate the interpretation of imaging studies compared with normal rats ($n = 15$). Quantitative MRI, including diffusion tensor imaging (DTI) and magnetization transfer imaging (MTI), and immunohistochemistry (IHC) analysis were used to examine the injury pattern up to 8 days post-injury in MVM and normal rats. Prior to injury, the MVM brain showed significant higher mean diffusivity, axial diffusivity, and radial diffusivity, and lower fractional anisotropy (FA) and magnetization transfer ratio (MTR) in the corpus callosum than normal brain ($p < 0.05$). Following TBI, normal brains exhibited significant decreases of FA in the corpus callosum, whereas MVM brains demonstrated insignificant changes in FA, suggesting less axonal injury. At day 8 after mild TBI, MTR of the normal brains significantly decreased whereas the MTR of the MVM brains significantly increased. IHC staining substantiated the MRI findings, demonstrating limited axonal injury with significant increase of microgliosis and astrogliosis in MVM brain compared with normal animals. The radiological-pathological correlation data showed that both DTI and MTI were sensitive in detecting mild diffuse brain injury, although DTI metrics were more specific in correlating with histologically identified pathologies. Compared with the higher correlation levels reflecting axonal injury pathology in the normal rat mild TBI, the DTI and MTR metrics were more affected by the increased inflammation in the MVM rat mild TBI. Because MVM Wistar rats appear normal, there was a need to screen rats prior to TBI research to rule out the presence of ventriculomegaly, which may complicate the interpretation of imaging and IHC observations.

Keywords: animal studies; DTI; model of injury; rats; TBI

Introduction

A consistent animal model of experimental traumatic brain injury (TBI) is crucial for the assessment of new diagnostic or therapeutic interventions. In TBI research, the Wistar albino rat is one of the most popular laboratory animals. Nearly 20% of the rat studies in the past decade used Wistar rats; > 123,129 research articles to date have been published associated with Wistar rats, according to the United States National Library of Medicine's PubMed database.

Spontaneous mild ventriculomegaly (MVM) was previously noted on baseline MR scans of Wistar rats used in a recent TBI study.[1] A total of 43% of the Wistar rats purchased from two different vendors had abnormalities in their ventricular and vascular systems in the brain. The patterns of congenital ventriculomegaly included mild to moderate ventricle dilation, scattered intracranial arachnoid cysts (in both gray and white matter), and, more rarely, necrotic paraflocculus and cerebellum. Spontaneous ventriculomegaly was also associated with abnormal vasculature, including aneurysms and arteriovenous malformations.[1] MVM rats had no abnormalities in young adulthood (i.e., skull size or shape) and could not be distinguished phenotypically from the normal rats. However, compared with normal rats, MVM rats have a 20% thinner corpus callosum and significantly increased astrogliosis in the cortex, without significant differences in myelination.[1] The ventriculomegaly brains exhibited significant differences in

[1]Frank Laboratory, Radiology and Imaging Sciences, Clinical Center, [2]Acute Studies Core, National Institute of Neurological Disorders and Stroke, and [3]National Institute of Biomedical Imaging and Bioengineering, National Institutes of Health, Bethesda, Maryland.

diffusion tensor imaging (DTI) metrics, which have been reported to be sensitive to diffuse axonal injury (DAI) in TBI patients[2,3] and in experimental studies.[4,5] At baseline, MVM rats have decreased fractional anisotropy (FA) and increased mean diffusivity (MD), axial diffusivity (AD), and radial diffusivity (RD) in the corpus callosum when compared with normal Wistar rats.

The purpose of this study was to investigate whether MVM rats exhibited different injury patterns after mild TBI in comparison with normal animals. Quantitative *in vivo* MRI techniques, including DTI and magnetization transfer imaging (MTI), were used and compared with immunohistochemistry (IHC) analysis to investigate the injury response between the normal and MVM rats following TBI. Careful consideration and baseline imaging studies should be performed in Wistar rats prior to inclusion in mild TBI experimental studies because the observations may conflate and skew results toward less primary axonal injury yet increased inflammation.

Methods

Ventriculomegaly rats and mild TBI

All studies were approved by the Institutional Animal Care and Use Committee at our institution, and experiments were performed according to the National Research Council's Guide for the Care and Use of Laboratory Animals. Female 8-week-old Wistar rats purchased from Charles River Laboratory (Wilmington, MA) and Harlan Laboratory (Indianapolis, IN) were used in this study. Rats underwent baseline MRI screening for patterns of ventriculomegaly by T2-weighted (T2W) images: TR 3.8 sec, TE 15 ms, rapid imaging with refocused echoes (RARE) factor 8, in-plane resolution 100×100 (μm) with 0.5 mm thickness using a Bruker 7T scanner (Bruker Corp., Billerica, MA) with a Doty radiofrequency quadrature coil (Doty Scientific, Inc., Columbia, SC). Thirty slices were acquired to cover the brain from olfactory bulb to cervical spinal cord to screen for ventriculomegaly. Each animal's baseline MRI was reviewed and scored at 8 anatomical locations to evaluate ventricular dilatation, asymmetrical ventricles, aqueduct stenosis, arachnoid cysts, cyst-like lesions, hyperintense lesions, and otherwise unidentified bright objects (UBO) per our previous guidelines.[1] Fifteen rats were identified with MVM, with an average score of 12.7 ± 4.8 on the ventriculomegaly rating scale (0–2: normal; 3–30: abnormal), and selected for the subsequent mild TBI study. Fifteen rats identified as within the normal limits served as the experimental controls.

Normal ($n = 10$) and MVM ($n = 10$) rats underwent a modified version of the Marmarou weight drop closed head injury model for mild TBI.[6] Isoflurane-anesthetized rats were placed on Marmarou polyurethane foam (density: 13.8 kg m^{-3}; Foam to Size Inc., Ashland, VA) with dimensions of 15 cm (H) $\times$20 cm (W) $\times$45 cm (L) to absorb excessive momentum. A custom- made metal disk was strapped to the top of the head to prevent skull fractures. A 450 g weight was allowed to free fall in a tube from distance of 2 m. Rats were monitored post-injury until they awakened and could move normally. Rats typically recovered within 5 min of impact. Five animals without injury served as the baseline controls for each group.

In vivo *MRI and data analysis*

In vivo MRI was conducted on animals prior to injury (baseline), and at 1 and 8 days post-injury (DPI). Animals were anesthetized with an isoflurane/oxygen mixture (4.5–5% for induction and 1.5–2.0% for maintenance). The inhalant anesthetic was delivered to the animal through a custom-made nose cone. Throughout MR scans, warm water was circulated through heating pads placed under the animals to keep them warm at 37°C. Respiratory rate was monitored using a pressure sensor (SA Instruments Inc., Stony Brook, NY) and maintained at 40–50 breaths per minute by an isoflurane/oxygen mixture.

At each time point, T2*-weighted images were first acquired to evaluate the presence of hemorrhage or subdural hematoma using three-dimensional (3D) multiple gradient echo (MGE): TR 60 ms, TE 3.18 ms, echo spacing 3.25 ms, voxel size 200 μm (isotropic). T2* maps were created by fitting the magnitude images of 14 echo MGE data to an exponential function on a pixel-by-pixel basis. DTI data was acquired using 3D spin echo echo-planar imaging (EPI) sequence with TR 700 ms, TE 37 ms; segment 4, Δ 15 ms; δ 5 ms; b-value 0 and 800 s/mm^2, 15 diffusion encoding directions. The voxel size of DTI was identical with MGE. Diffusion-weighted images were corrected for B_0 susceptibility-induced EPI distortion, eddy current distortions, and motion distortion with b-matrix reorientation using Tortoise.[7]

After correction, the diffusion tensor was calculated to derive DTI parameters, including FA, MD, AD, and RD. MTI was acquired by two dimensional (2D) RARE sequence with (M_S) and without (M_0) magnetic transfer (MT) preparation pulses added before excitation: TR 5000 ms, TE 11.56 ms, RARE factor 8, MT saturation frequency offsets 6000 Hz, saturation pulse amplitude 4 μT, duration 1 ms, pulse number 20, pixel size 200 μm^2, and slice thickness 0.5 mm.

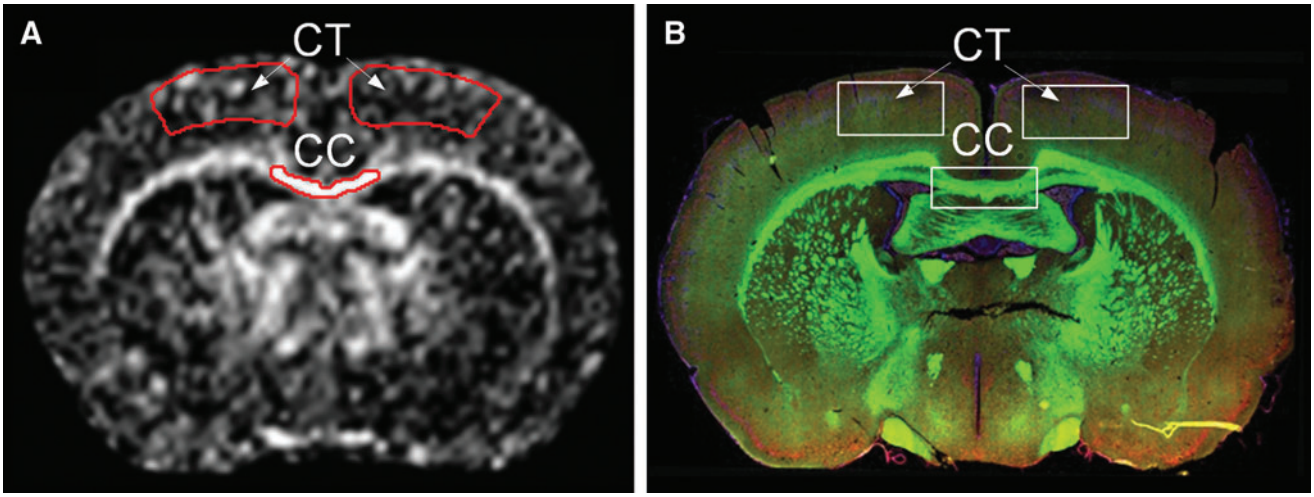

FIG. 1. The MRI **(A)** and immunohistochemistry **(B)** data were acquired from the regions of interest at bregma −1.0 mm. CC, corpus callosum; CT, cortex. Color image is available online at www.liebertpub.com/neu

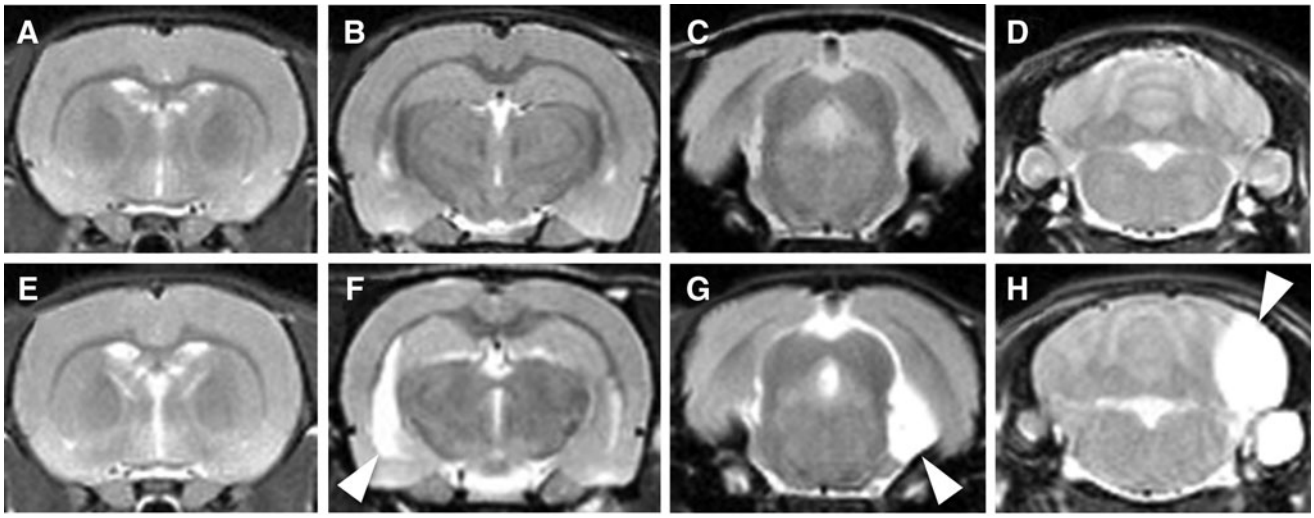

FIG. 2. Representative anatomical T2-weighted images from normal **(A–D)** and mild ventriculomegaly **(E–H)** rats. Clear asymmetric lateral ventricle **(F)**, arachnoid cyst **(G)**, or unidentified bright object bright objects **(H)** may be found in the ventriculomegaly brain.

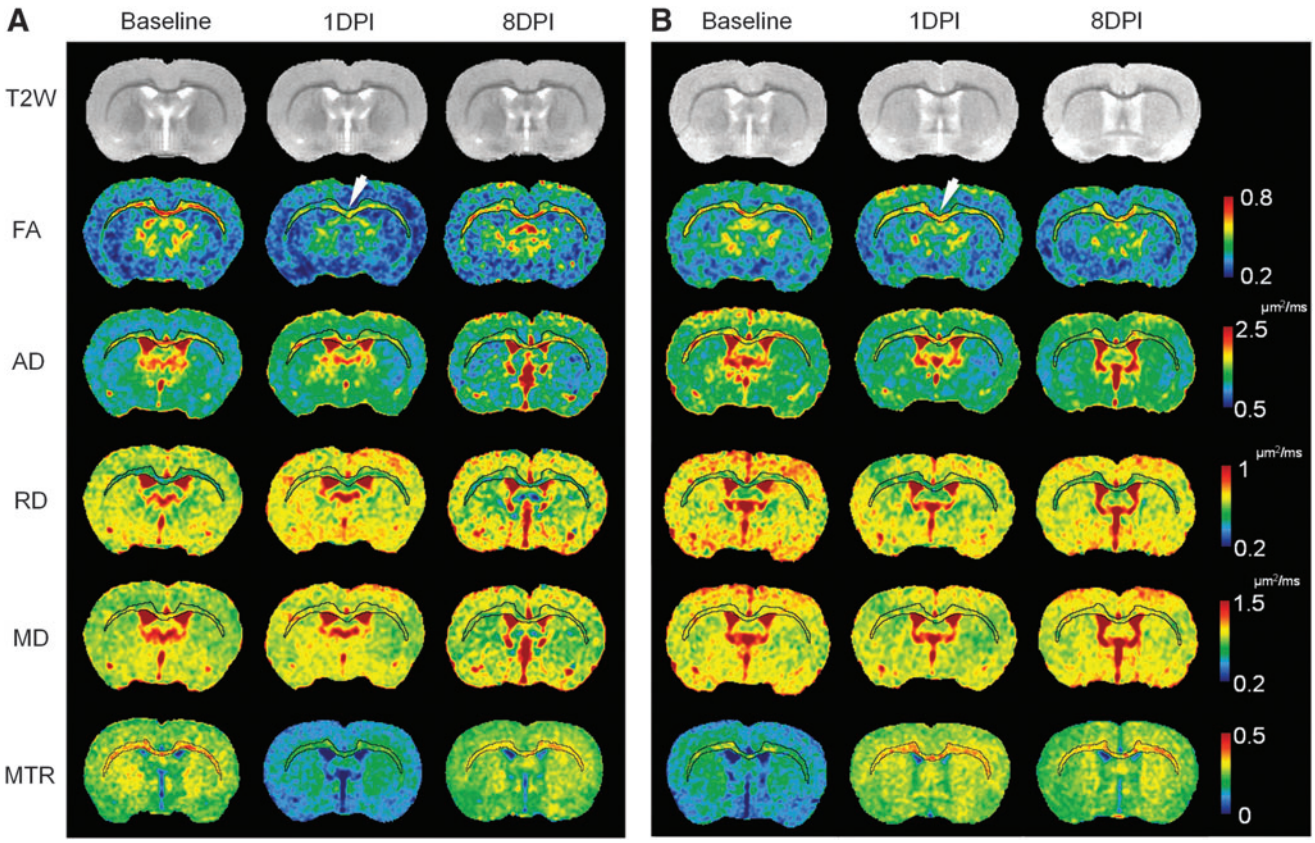

FIG. 3. Longitudinal diffusion tensor imaging (DTI) and magnetization transfer ratio (MTR) maps of the normal **(A)** and mild ventriculomegaly (MVM) **(B)** brain following mild traumatic brain injury (TBI). Corpus callosum and external capsule were segmented to highlight the pattern of diffuse axonal injury over time. Decreases of fractional anisotropy (FA) (arrow in **A**), axial diffusivity (AD), and MTR were clearly seen immediately after injury in the normal brain at 1 day post-injury (DPI), whereas radial diffusivity (RD), and mean diffusivity (MD) show changes and were scattered across multiple locations. MVM rat brains do not show the similar axonal injury pattern in the FA maps at 1 DPI (arrow in **B**). The MTR maps show dramatic different trends of contrast changes in the ventriculomegaly brain in response to mild TBI. Color image is available online at www.liebertpub.com/neu

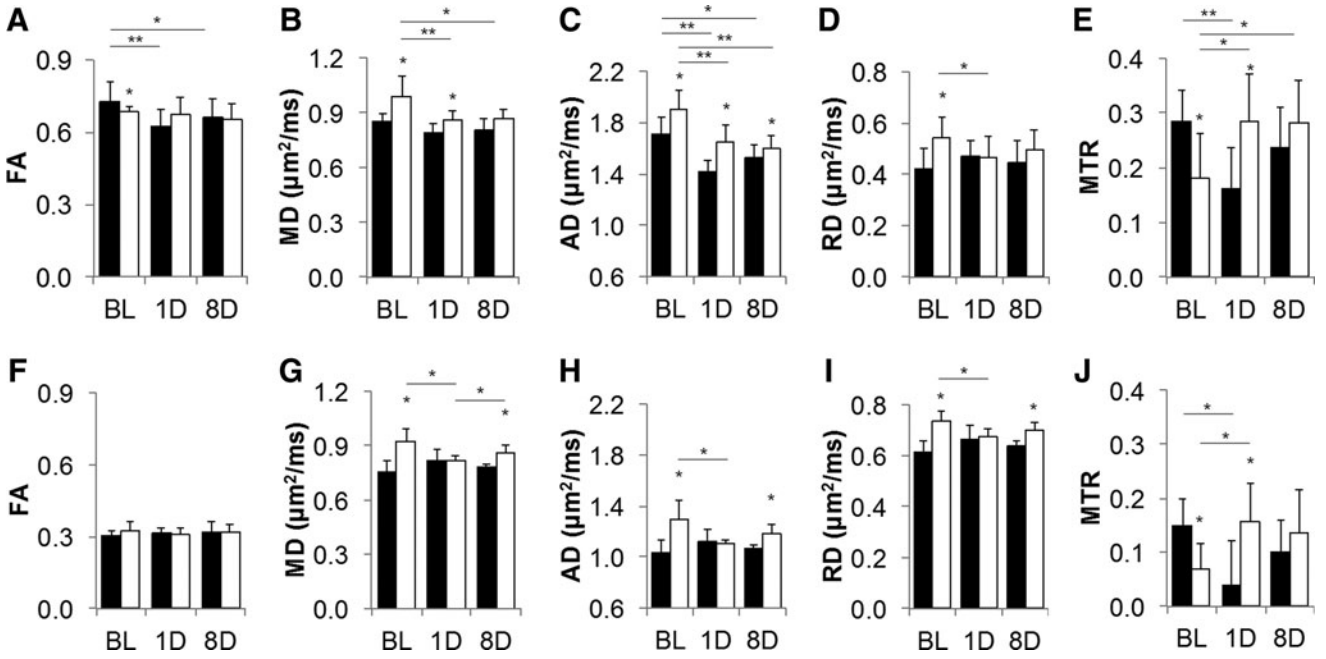

FIG. 4. Mean values of the diffusion tensor imaging (DTI) and magnetization transfer imaging (MTI) metrics obtained from the corpus callosum **(A–E)** and cerebral cortex **(F–J)** of the normal (■) and mild ventriculomegaly (MVM) (□) rats following mild traumatic brain injury (TBI) over time. DTI and MTI metrics reveal different injury response between the normal and MVM rats following mild TBI. $*p < 0.05$, $**p < 0.01$.

Magnetization transfer ratio (MTR) maps were calculated by $(M_0\text{-}M_S)/M_0$. Region of interest (ROI) analysis was performed using ImageJ (NIH, Bethesda, MD) on the corpus callosum and cortex near Bregma −1.0 mm, which was previously identified as the location showing the most DAI in this injury model (Fig. 1). ROIs were manually defined on three consecutive imaging slices for the DTI data set using the FA maps and on one slice for the MTR maps. Values of DTI and MTI metrics were acquired and then averaged to be the final values. A voxel-by-voxel temporal-spatial statistical analysis was performed for the FA and MTR maps to test the sensitivity and specificity of examining the microstructural abnormalities in the entire brain over the 8 day period following mild TBI. FA and MTR maps were segmented and registered to a common space of an anatomical image using FLIRT[8] and TBSS.[9] Each of the rats' aligned maps were projected onto the mean skeleton, and the resulting data fed into voxelwise cross-subject statistics by repeated measures analysis of variance (ANOVA).[9] The null distribution for the data in the TBSS statistics was built over 10,000 permutations, and the results were shown as a voxelwise significance level (p value) <0.05. For the multiple comparison correction within the data, cluster-level inference at $t > 2.7$, $p < 0.05$, and false discovery rate theory[10] at $q < 0.05$ were used. Except for those processed by the aforementioned software, all other imaging data were processed via in house Matlab (Mathwork, Natick, MA) programs.

IHC analysis

Five rats per group were randomly picked for IHC examination at each imaging time point following MRI. Following euthanasia, animals were perfused with 4% paraformaldehyde in phosphate-buffered saline (PBS) for histology. The brain tissue was cryosectioned at 10 μm for IHC staining. Slides of sectioned tissue were washed with PBS, blocked in Superblock (Scy Tek Laboratories, Logan, UT) for 10 min at room temperature, and incubated in primary antibody to detect activated microglia, ionized calcium-binding adaptor molecule 1 (Iba1) (Wako, Richmond, VA) at 1/200; astrocytes, glial fibrillary acidic protein (GFAP) (Abcam, Cambridge, MA) at 1/1500; phosphorylated neurofilament H (SMI31) (Covance, Princeton, NJ) at 1/1500; myelin basic protein (MBP) (Abcam, Cambridge, MA) at 1/500 in 1x PBS, 0.3% Tween-20, and 1.0% bovine serum albumin at 4°C overnight. After three PBS +0.3% Tween-20 washes, slices were incubated in secondary antibody: for MBP and SMI31, goat F(ab') polyclonal secondary antibody to mouse IgG- H&L Dylight 594 (Abcam, Cambridge, MA); for Iba1 and GFAP, goat anti-rabbit F(ab') IgG-H&L Dylight 594 (Abcam, Cambridge, MA) at a dilution of 1/200 in 1x PBS with 0.3% Tween-20 and 1.0% bovine serum albumin at room temperature for 1 h, rinsed three times in PBS +0.3% Tween-20, dipped in dH2O, and mounted in ProLong Gold antifade with 4',6-diamidino-2-phenylindole (DAPI) (Invitrogen, Carlsbad, CA). Slides were visualized with an Aperio FL fluorescent microscope (Aperio, Vista, CA). The quantification of IHC staining was conducted by counting the areas of the positive staining in the 20× images using Matlab program CellC with manual confirmation.[11]

Statistical analysis

Statistical analysis was conducted using Prism software version 6.0c (GraphPad Software, Inc., La Jolla, CA). Longitudinal data were analyzed using two way ANOVA with repeated measures. Bonferroni correction for multiple comparisons was used to examine the difference between normal and MVM rats, with significance levels predetermined at 0.05. Pearson correlation analysis was performed to delineate the possible pathological correlation between the MRI and IHC data. All data are reported as mean ± standard deviation (SD).

Results

Abnormal patterns of mild to moderate ventriculomegaly were detected in MVM Wistar rats on anatomical T2W MRI (Fig. 2). Compared with normal brain, morphological changes of MVM-affected brains include ventriculomegaly, white matter cysts, and

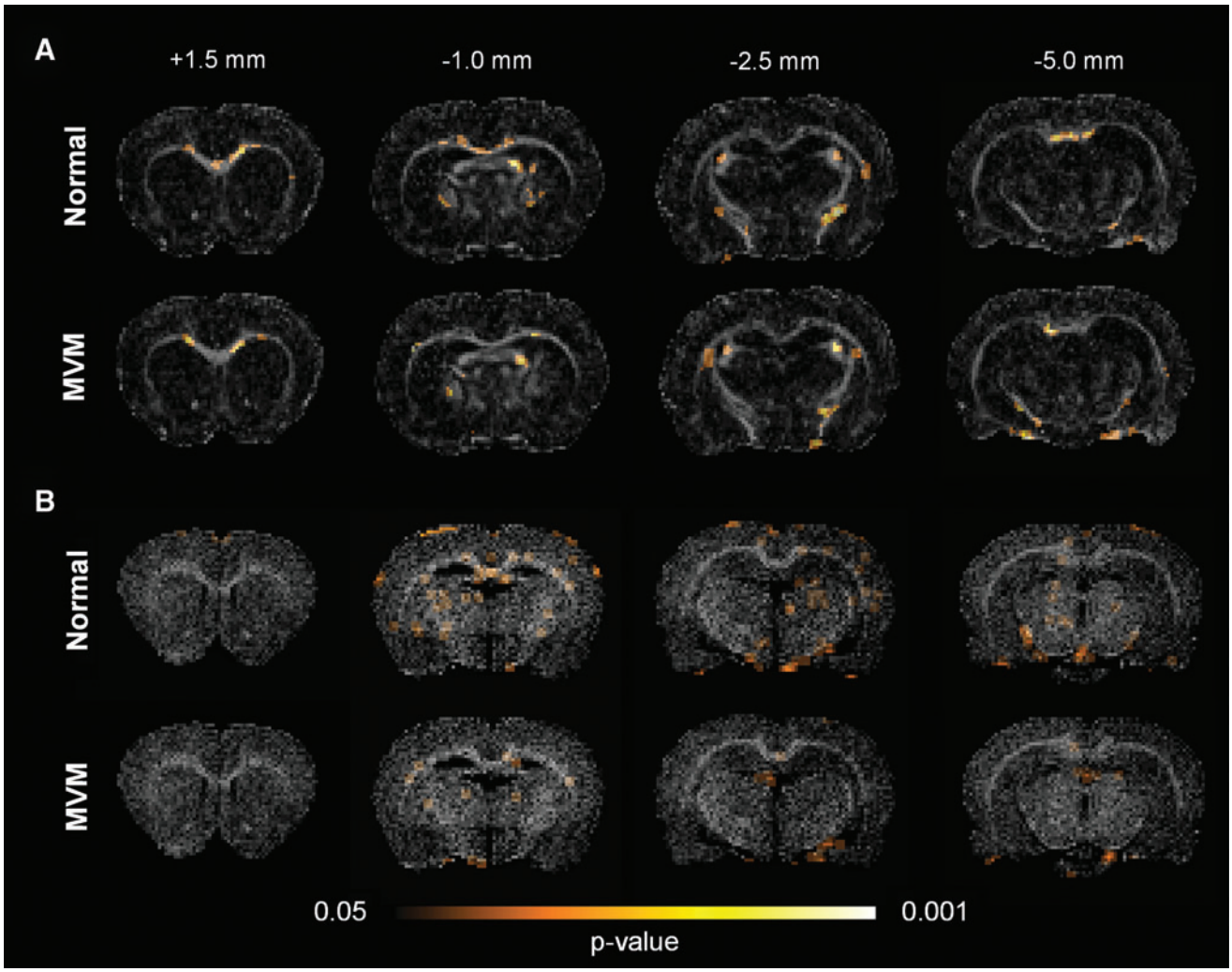

FIG. 5. The significance maps of the fractional anisotropy (FA) **(A)** and magnetization transfer ratio (MTR) **(B)** reveal the temporal-spatial difference of the injury patterns between the normal and mild ventriculomegaly (MVM) rats over a period of 8 days following mild traumatic brain injury (TBI). Both FA and MTR detect more severe injury in the normal rats toward the genu of the corpus callosum, whereas the injury in the MVM rats was less prominent over the entire brain. Color image is available online at www.liebertpub.com/neu

UBOs in various locations. Figure 3 compares MRIs between normal and MVM brains after mild TBI over time. Although T2W images were qualitatively indistinguishable between normal (Fig. 3A) and MVM (Fig. 3B) rats following mild TBI, DTI and MTI detected significant differences between the two groups in response to mild TBI. Sequential FA maps revealed significant loss of contrast in the corpus callosum of normal brain at 1 DPI, but not in MVM brain (Fig. 3B). MTR maps of normal and MVM brains displayed different trends in response to mild TBI, with clear changes at baseline and 1 DPI.

The mean values of DTI and MTI metrics acquired from the corpus callosum and cortex are presented in Figure 4. On baseline scans, MVM brains exhibited significantly ($p < 0.05$) higher AD, RD, and MD in both corpus callosum (Fig. 4 A–E) and cortex (Fig. 4 F–J) when compared with normal rats. FA in MVM rats was significantly ($p < 0.05$) lower in the corpus callosum, but not in the cortex (Fig. 4 A, F). MTR for both the corpus callosum and the cortex was significantly lower ($p < 0.05$) in the baseline of MVM rats (Fig. 4 E, J). Following mild TBI, normal brain demonstrated significant decreases ($p < 0.01$) in FA and AD in the corpus callosum at 1 DPI, whereas RD and MD only showed slight increases in multiple spots without significance. In comparison, in MVM rats, AD, RD, and MD were significantly decreased ($p < 0.05$) after injury; however, FA was similar to baseline values. DTI from normal cortex demonstrated slight increases in AD, RD, and MD at 1 DPI, returning to the baseline levels at 8 DPI, whereas that of MVM rats showed significant decreases ($p < 0.05$) at 1 DPI. For both groups, FA did not change in the cortex following mild TBI over time. MTR showed prominent contrasting patterns between normal and MVM rats. In the normal corpus callosum, MTR significantly decreased ($p < 0.01$) at 1 DPI, which normalized to baseline levels at 8 DPI (Fig. 4E). However, MTR significantly increased ($p < 0.05$) at 1 DPI, and remained high at 8 DPI in MVM corpus callosum. Similar MTR changes were also seen in the cortex, except for the insignificant increase of MTR between baseline and 8 DPI for MVM brains (Fig. 4J). A distinct pattern of abnormalities existed in the voxelwise statistical map of FA and MTR between the normal and MVM rats related to mild TBI over a period of 8 DPI (Fig. 5). Significant changes were more evident in both FA and MTR maps of the normal brain than in those of the

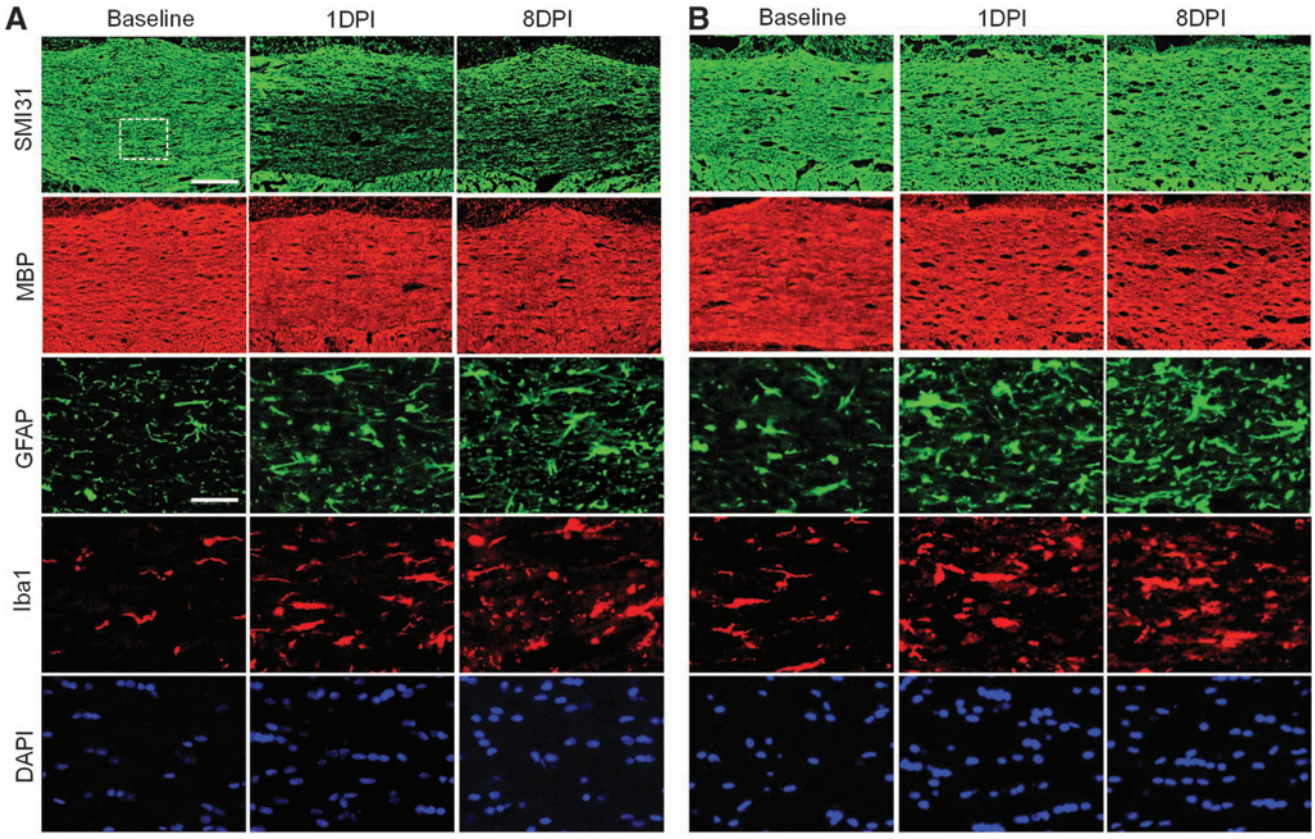

FIG. 6. Representative images of the immunofluorescent staining of the corpus callosum in the normal **(A)** and mild ventriculomegaly **(B)** brain after mild traumatic brain injury (TBI). Fluorescent micrographs of glial fibrillary acidic protein (GFAP), ionized calcium-binding adaptor molecule 1 (Iba1), and 4',6-diamidino-2-phenylindole (DAPI) images were taken from the region denoted in the SMI31 image. Scale bar: 200 μm for SMI31 and MBP; 50 μm for GFAP, Iba1 and DAPI. Color image is available online at www.liebertpub.com/neu

MVM brain following mild TBI over time, especially in the corpus callosum near Bregma −1.0 mm.

Figure 6 displays the serial IHC photomicrographs of the corpus callosum between normal and MVM brains. Figure 7 shows the quantitative data from the IHC staining. Following mild TBI, SMI31 staining showed significant axonal injury in the corpus callosum of normal rats at 1 DPI and 8 DPI, whereas axonal injury was not clearly detected in MVM corpus callosum (Figs. 6 and 7A). MBP staining did not reveal significant loss of myelin, with only patchy loss in the corpus callosum observed for both cohorts over time (Figs. 6 and 7B). Comparing to the normal brain, the MVM brain showed significant higher amounts of Iba1 staining at baseline (Fig. 6 and 7C). After injury, both groups exhibited progressively increased microgliosis, whereas MVM rats had nearly 40%

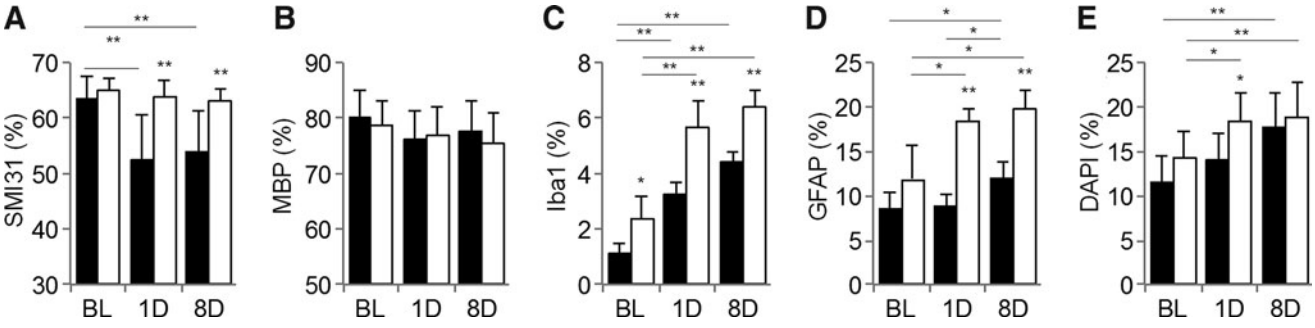

FIG. 7. Quantification of immunohistochemistry for SMI31 **(A)**, myelin basic protein (MBP) **(B),** ionized calcium-binding adaptor molecule 1 (Iba1) **(C)**, glial fibrillary acidic protein (GFAP) **(D)**, and 4',6-diamidino-2-phenylindole (DAPI) **(E)** in the corpus callosum of normal (■) and ventriculomegaly (□) rats. SMI31 staining clearly demonstrates the loss of axonal staining at 1 day post-injury (DPI) and 8 DPI in the normal brain, whereas no significant changes in the axonal staining are seen in the ventriculomegaly brain **(A)**. After injury, there is no significant loss of myelin by MBP staining in either group **(B)**. Iba1 **(C)** and GFAP **(D)** show the increasing trend of microgliosis and astrogliosis, whereas excessively more Iba1 and GFAP-positive staining are shown in the ventriculomegaly brain. DAPI staining shows that both groups experience increased cellularity following mild traumatic brain injury, but the cellularity in the ventriculomegaly brain is significantly greater than that in the normal brain at 1 DPI. $*p<0.05$, $**p<0.01$.

Table 1. Pathological Correlation of the DTI and MTR Metrics versus Histological Quantification

IHC	*Group*	*FA*	*MD*	*AD*	*RD*	*MTR*
SMI31	Normal	**0.73**	0.35	**0.71**	–0.43	0.23
	MVM	0.33	0.01	0.03	–0.22	–0.02
MBP	Normal	–0.26	–0.11	–0.11	0.09	0.30
	MVM	–0.12	0.39	0.53	0.34	–0.55
DAPI	Normal	–0.52	–0.47	**−0.65**	0.49	–0.33
	MVM	–0.02	–0.54	**−0.75**	–0.36	**0.67**
Iba1	Normal	–0.57	–0.39	–0.54	**0.65**	–0.39
	MVM	–0.21	–0.48	**−0.72**	–0.22	**0.68**
GFAP	Normal	–0.35	–0.07	–0.28	–0.06	0.56
	MVM	0.07	**−0.76**	**−0.78**	–0.54	**0.71**

Bold characters mark the correlations with significant level <0.05.

DTI, diffusion tensor imaging; MTR, magnetization transfer ratio; IHC, immunohistochemistry; FA, fractional anisotropy; MD, mean diffusivity; AD, axial diffusivity; RD, radial diffusivity; MBP, myelin basic protein; DAPI, 4′,6-diamidino-2-phenylindole; Iba1, ionized calcium-binding adaptor molecule 1; GFAP, glial fibrillary acidic protein; MVM, mild ventriculomegaly.

more Iba1-positive staining area than normal rats. Significant increases in GFAP staining were detected in normal brains at 8 DPI, whereas MVM brains showed significant increases in GFAP since 1 DPI (Figs. 6 and 7D). Cellularity by DAPI staining was significantly higher in the MVM rats at 1 DPI following injury (Figs. 6 and 7E). The radiological-pathological correlation analysis revealed that the DTI and MTR metrics correlated with the IHC identified pathology in mild TBI (Table 1). FA and AD detected more severely axonal injury in the normal rat TBI, where the changes in MD, AD, and MTR correlated with the increased inflammation in the MVM rat TBI.

Discussion

The Wistar albino rat is one of the most popular experimental animals used in biomedical research because of ease of breeding and husbandry along with the existence of large databases for comparing results.[12] Although most of these studies assumed a consistent baseline condition of animals, the current study indicates that there may be inherent morphological variability among Wistar rats that could lead to misinterpretation of results if not culled out or appropriately randomized prior to experimental injury or therapeutic intervention.[13]

Compared with normal brains, significantly increased baseline AD, RD, and MD, and decreased FA and MTR were found in the MVM brain corpus callosum (Fig. 4). These phenomena may result from increased water content and fewer barriers in the MVM brain parenchyma to water diffusion,[14] accompanied by fewer nonaqueous molecules to exchange magnetization with water.[15] The myelinated axons might also have been spread apart by the increased water content,[15] as more noncellular spaces were detected in the MVM brain tissue by histology (Fig. 6B). In addition, increased astrogliosis and microgliosis were observed in MVM rats than in normal rats at baseline (Figs. 6 and 7), suggesting an ongoing sterile inflammatory response that might be related to ventriculomegaly.[16] Further proteomic investigation beyond the scope of the current study would be needed to determine if there were proinflammatory cytokines or chemokines present in the parenchyma that were driving the observed histological differences between the two cohorts.[17] Following mild TBI, MVM rats demonstrated less primary axonal injury with insignificant changes of FA and neurofilament staining at 1 DPI compared with baseline (Fig. 6). At 8 DPI, histology elevated activated microgliosis and astrogliosis were clearly observed in the MVM rats compared with normal rats. The significantly decreased AD and increased RD from 1 DPI to 8 DPI in MVM rats were consistent with increased inflammation, instead of axonal injury (Table 1).[18] The decreased MD and increased MTR by 8 DPI in the corpus callosum and cortex of injured MVM brains suggest resolution of post-injury edema.[14,15]

The radiological-pathological correlation analysis affirmed that FA and AD primarily reflected the axonal damage in DAI, but could also be altered by the microgliosis and increased cellularity during the secondary injury stage (Table 1).[4,5] Without profound demyelination in the current mild TBI model (Figs. 6 and 7), RD displayed a strong reaction to the increased microgliosis, and was partially associated with axonal integrity, increased cellularity and likely the presence of edema (Table 1). In the gray matter of injured normal rats, both AD and RD increased after 1 DPI because of edema and presumed membrane destruction, whereas by 8 DPI, there was less edema present in the parenchyma, and these metrics better reflected tissue integrity (Figs. 3 and 4). In contrast, post-injury MVM brains displayed deviation of the pattern of DTI metrics from the normal brain TBI, and showed higher correlations to the increased cellularity, microgliosis, and astrogliosis following mild TBI. These results suggest that DTI metrics were sensitive and specific to DAI in the acute phase. Nevertheless, the changes of DTI metrics were also affected by the increased inflammatory mild TBI pathology. The change of water content and fewer barriers to water diffusion in the MVM brains may also significantly alter the DTI measurements.

Radiological-pathological correlation also demonstrated that increases in astrogliosis and microgliosis had more effects than the axonal integrity on the changes of MTR in the presence of limited demyelination (Table 1). However, the MTR changes in the MVM injured rats were probably associated with other unknown mechanisms related to the rapid resolution of water content in the MVM brains following injury.[19,20] Because significant increases of astrocytes were found in the MVM rats over the entire brain,[1] we speculate that it is possible that aquaporin 4 water channels were increased on astrocytes to remove the interstitial water and decrease the water content.[19–22] Further investigation is required to understand the mechanism for generating different MTR contrast in the MVM animals.

The voxelwise statistical maps allow visualization of the spatial patterns of FA and MTR changes across all of the injured animals compared with the baseline images (Fig. 5). The temporal-spatial changes in FA and MTR were more distinguishable in the normal brain than in the MVM brain, suggesting more severe patterns of DAI in the normal rats following mild TBI. Although the underlying mechanism for abnormal injury responses in MVM rats following mild TBI is unknown, a possible hypothesis is that the presumable increased water content in these animals could contribute to decreased brain stiffness making it less susceptible to injury.[23–25] In contrast, MVM rats manifested more activated microglia after injury, perhaps indicating an enhanced immunological response in these animals. Previous studies documented enhanced microgliosis and astrogliosis in the hydrocephalic brain similar to the results in the current study.[26–30] IHC staining revealed excessive gliosis existing around the vessels and dilated ventricles that was associated with the increase of FA in MVM rats compared with

controls. We speculate that the increased density of astrocytes and microglia around the hydrocephalic ventricles and vessels in the MVM rat could contribute to inflammatory responses that could alter the blood–brain barrier (BBB) integrity, impair cerebral perfusion, impede neuronal plasticity, and change intracranial compliance.[31] Ventriculomegaly has also been found to cause injury to periventricular axons and microvessels, and to induce delayed demyelination.[32,33] Moreover, agenesis and dysgenesis of the corpus callosum were also reported to account for the formation of arachnoid cysts from the extension of pre-existing ventriculomegaly and hydrocephalus in interhemispheric fissure.[34–36]

In the current study, MVM rats were phenotypically indistinguishable from normal animals. T2W images revealed a communicating hydrocephalus, characterized by mild ventriculomegaly, with various types of cysts or hyperintensive lesions without evidence of aqueduct stenosis. Although the DTI and MTR measure a macroscopic effect observed with multiple types of pathology, the differences in DTI metrics and MTR between MVM and normal rats may not reliably reflect white matter integrity. The inclusion of MVM animals in TBI studies may confound interpretation of imaging results. An unbalanced distribution of MVM with normal rats in experimental TBI studies would introduce a large variation on the primary axonal injury severity and dilute the effectiveness of MRI metrics in depicting the degree of injury or recovery over time. Although recent criticism has been made as to whether rodents accurately recapitulate clinical experience, rodents are still the most commonly used species for the experimental modeling of neurological diseases.[37] This current study underscores the importance of baseline imaging studies to characterize morphology prior to conducting experimental studies. Appropriate balanced distribution or segregation of MVM animals from TBI studies based on imaging studies would reinforce and strengthen potential clinical and pathological observations, and be more reflective of the general clinical population. Nevertheless, MVM Wistar rats could represent a novel model for studying spontaneous ventriculomegaly in association with cyst formation.

Conclusion

In the current study, we have shown that the normal appearing MVM rats exhibited milder axonal injury in association with greater amounts of astrogliosis and microgliosis following mild TBI than did normal rats. Both DTI and MTR are sensitive in detecting mild diffuse brain injury, although DTI metrics were more specific in correlating with histologically identified neuropathologies. Compared with the higher correlation levels reflecting axonal injury pathology in the normal rat mild TBI, the DTI and MTR metrics were more affected by the increased inflammation in the MVM rat with mild TBI. Baseline scans are strongly suggested if animals that exhibit ventriculomegaly are to be included in experimental studies. Adjustments to sample sizes and randomization paradigms may be necessary, especially when MRI metrics are to be used as primary outcome measures in the evaluation of novel therapeutic interventions in neurological disease models.

Acknowledgments

This work was supported by funding from the Department of Defense through the Center for Neuroscience and Regenerative Medicine (Henry M. Jackson Foundation Awards #300604-8.01-60855 and #305500-8.01-60855) and from the Intramural Research Programs of the Clinical Center and of the National Institute of Biomedical Imaging and Bioengineering at the National Institutes of Health.

Author Disclosure Statement

No competing financial interests exist.

References

1. Tu, T.W., Turtzo, L.C., Williams, R.A., Lescher, J.D., Dean, D.D., and Frank, J.A. (2014). Imaging of spontaneous ventriculomegaly and vascular malformations in Wistar rats: implications for preclinical research. J. Neuropathol. Exp. Neurol. 73, 1152–1165.
2. Rutgers, D.R., Toulgoat, F., Cazejust, J., Fillard, P., Lasjaunias, P., and Ducreux, D. (2008). White matter abnormalities in mild traumatic brain injury: a diffusion tensor imaging study. AJNR Am J Neuroradiol 29, 514–519.
3. Veeramuthu, V., Narayanan, V., Kuo, T.L., Delano–Wood, L., Chinna, K., Bondi, M.W., Waran, V., Ganesan, D., and Ramli, N. (2015). Diffusion tensor imaging parameters in mild traumatic brain injury and its correlation with early neuropsychological impairment: a longitudinal study. J. Neurotrauma 32, 1497–1509.
4. Li, J., Li, X.Y., Feng, D.F., and Gu, L. (2011). Quantitative evaluation of microscopic injury with diffusion tensor imaging in a rat model of diffuse axonal injury. Eur. J. Neurosci. 33, 933–945.
5. Laitinen, T., Sierra, A., Bolkvadze, T., Pitkanen, A., and Grohn, O. (2015). Diffusion tensor imaging detects chronic microstructural changes in white and gray matter after traumatic brain injury in rat. Front. Neurosci. 9, 128.
6. Marmarou, A., Foda, M.A., van den Brink, W., Campbell, J., Kita, H., and Demetriadou, K. (1994). A new model of diffuse brain injury in rats. Part I: Pathophysiology and biomechanics. J. Neurosurg. 80, 291–300.
7. Irfanoglu, M.O., Machiraju, R., Sammet, S., Pierpaoli, C., and Knopp, M.V. (2008). Automatic deformable diffusion tensor registration for fiber population analysis. Med. Image Comput. Comput. Assist. Interv. 11, 1014–1022.
8. Jenkinson, M., and Smith, S. (2001). A global optimisation method for robust affine registration of brain images. Med. image Anal. 5, 143–156.
9. Smith, S.M., Johansen–Berg, H., Jenkinson, M., Rueckert, D., Nichols, T.E., Miller, K.L., Robson, M.D., Jones, D.K., Klein, J.C., Bartsch, A.J., and Behrens, T.E. (2007). Acquisition and voxelwise analysis of multi-subject diffusion data with tract-based spatial statistics. Nat. Protoc. 2, 499–503.
10. Genovese, C.R., Lazar, N.A., and Nichols, T. (2002). Thresholding of statistical maps in functional neuroimaging using the false discovery rate. NeuroImage 15, 870–878.
11. Selinummi, J., Seppala, J., Yli-Harja, O., and Puhakka, J.A. (2005). Software for quantification of labeled bacteria from digital microscope images by automated image analysis. Biotechniques 39, 859–863.
12. Kacew, S., and Festing, M.F. (1996). Role of rat strain in the differential sensitivity to pharmaceutical agents and naturally occurring substances. J Toxicol. Environ. Health 47, 1–30.
13. Turtzo, L.C., Budde, M.D., Gold, E.M., Lewis, B.K., Janes, L., Yarnell, A., Grunberg, N.E., Watson, W., and Frank, J.A. (2013). The evolution of traumatic brain injury in a rat focal contusion model. NMR Biomed. 26, 468–479.
14. Tu, T.W., and Frank, J.A. (2013). Assessing white matter integrity in experimental spinal cord injury using diffusion tensor imaging. J. Neurosci. Neuroeng. 2, 415–430.
15. Vavasour, I.M., Laule, C., Li, D.K., Traboulsee, A.L., and MacKay, A.L. (2011). Is the magnetization transfer ratio a marker for myelin in multiple sclerosis? J Magn. Reson. imaging 33, 713–718.
16. Chen, G.Y., and Nunez, G. (2010). Sterile inflammation: sensing and reacting to damage. Nat. Rev. Immunol. 10, 826–837.
17. Gadani, S.P., Walsh, J.T., Lukens, J.R., and Kipnis, J. (2015). Dealing with danger in the CNS: the response of the immune system to injury. Neuron 87, 47–62.
18. Wang, Y., Wang, Q., Haldar, J.P., Yeh, F.C., Xie, M., Sun, P., Tu, T.W., Trinkaus, K., Klein, R.S., Cross, A.H., and Song, S.K. (2011). Quantification of increased cellularity during inflammatory demyelination. Brain 134, 3590–3601.
19. Papadopoulos, M.C., Manley, G.T., Krishna, S., and Verkman, A.S. (2004). Aquaporin-4 facilitates reabsorption of excess fluid in vasogenic brain edema. FASEB J 18, 1291–1293.

20. Tourdias, T., Dragonu, I., Fushimi, Y., Deloire, M.S., Boiziau, C., Brochet, B., Moonen, C., Petry, K.G., and Dousset, V. (2009). Aquaporin 4 correlates with apparent diffusion coefficient and hydrocephalus severity in the rat brain: a combined MRI-histological study. NeuroImage 47, 659–666.
21. Saadoun, S., Papadopoulos, M.C., Watanabe, H., Yan, D., Manley, G.T., and Verkman, A.S. (2005). Involvement of aquaporin-4 in astroglial cell migration and glial scar formation. J. Cell Sci. 118, 5691–5698.
22. Tourdias, T., Mori, N., Dragonu, I., Cassagno, N., Boiziau, C., Aussudre, J., Brochet, B., Moonen, C., Petry, K.G., and Dousset, V. (2011). Differential aquaporin 4 expression during edema build–up and resolution phases of brain inflammation. J. Neuroinflammation 8, 143.
23. Kuroiwa, T., Yamada, I., Katsumata, N., Endo, S., and Ohno, K. (2006). Ex vivo measurement of brain tissue viscoelasticity in post-ischemic brain edema. Acta Neurochir. Suppl. 96, 254–257.
24. Streitberger, K.J., Wiener, E., Hoffmann, J., Freimann, F.B., Klatt, D., Braun, J., Lin, K., McLaughlin, J., Sprung, C., Klingebiel, R., and Sack, I. (2011). In vivo viscoelastic properties of the brain in normal pressure hydrocephalus. NMR Biomed. 24, 385–392.
25. Boulet, T., Kelso, M.L., and Othman, S.F. (2013). Long-term in vivo imaging of viscoelastic properties of the mouse brain after controlled cortical impact. J. Neurotrauma 30, 1512–1520.
26. Eskandari, R., Harris, C.A., and McAllister, J.P., 2nd (2011). Reactive astrocytosis in feline neonatal hydrocephalus: acute, chronic, and shunt-induced changes. Childs Nerv Syst 27, 2067–2076.
27. Yoshida, Y., Koya, G., Tamayama, K., Kumanishi, T., and Abe, S. (1990). Development of GFAP-positive cells and reactive changes associated with cystic lesions in HTX rat brain. Neurol. Med. Chir. (Tokyo) 30, 445–450.
28. Khan, O.H., Enno, T.L., and Del Bigio, M.R. (2006). Brain damage in neonatal rats following kaolin induction of hydrocephalus. Exp. Neurol. 200, 311–320.
29. Deren, K.E., Packer, M., Forsyth, J., Milash, B., Abdullah, O.M., Hsu, E.W., and McAllister, J.P., 2nd (2010). Reactive astrocytosis, microgliosis and inflammation in rats with neonatal hydrocephalus. Exp. Neurol. 226, 110–119.
30. Del Bigio, M.R. (2001). Pathophysiologic consequences of hydrocephalus. Neurosurg. Clin. N. Am. 12, 639–649, vii.
31. Miller, J.M., and McAllister, J.P., 2nd (2007). Reduction of astrogliosis and microgliosis by cerebrospinal fluid shunting in experimental hydrocephalus. Cerebrospinal Fluid Res. 4, 5.
32. McAllister, J.P., 2nd (2012). Pathophysiology of congenital and neonatal hydrocephalus. Semin. Fetal Neonatal Med. 17, 285–294.
33. Jain–Ghai, S., Mishra, N., Hahn, C., Blaser, S., and Mercimek–Mahmutoglu, S. (2014). Fetal onset ventriculomegaly and subependymal cysts in a pyridoxine dependent epilepsy patient. Pediatrics 133, e1092–1096.
34. Schell–Apacik, C.C., Wagner, K., Bihler, M., Ertl–Wagner, B., Heinrich, U., Klopocki, E., Kalscheuer, V.M., Muenke, M., and von Voss, H. (2008). Agenesis and dysgenesis of the corpus callosum: clinical, genetic and neuroimaging findings in a series of 41 patients. Am. J. Med. Genet. Part A 146A, 2501–2511.
35. Noguchi, R., Abe, K., Hamada, H., Ogura, T., Obata, M., Miyazono, Y., and Yoshikawa, H. (2014). Outcomes of patients with prenatally diagnosed agenesis of the corpus callosum in conjunction with ventriculomegaly. Arch. Gynecol. Obstet. 290, 237–242.
36. Oh, K.Y., Kennedy, A.M., Selden, N.R., McLean, L., and Sohaey, R. (2012). Asymmetric ventriculomegaly, interhemispheric cyst, and dysgenesis of the corpus callosum (AVID): an imaging triad. J. Ultrasound Med. 31, 1811–1820.
37. Couzin–Frankel, J. (2013). When mice mislead. Science 342, 922–925.

Address correspondence to:
Tsang-Wei Tu, PhD
Radiology and Imaging Sciences
Clinical Center
National Institutes of Health
USA Building 10, RM B1N256
10 Center Drive MSC 1074
Bethesda, MD 20892

E-mail: tut@cc.nih.gov